Charge Transfer and Reactivity of $n\pi^*$ and $\pi\pi^*$ Organic Triplets, Including Anthraquinonesulfonates, in Interactions with Inorganic Anions: A Comparative Study Based on Classical Marcus Theory

I. Loeff,† J. Rabani,† A. Treinin,*,† and H. Linschitz*,‡

Contribution from the Department of Physical Chemistry and the Farkas Center for Light-Induced Processes, Hebrew University, Jerusalem 91904, Israel, and Department of Chemistry, Brandeis University, Waltham, Massachusetts 02254-9110

Received March 15, 1993

Abstract: The study of rates and radical yields in charge-transfer (CT) interactions between organic triplets and simple anions has been extended to triplets of 1-sulfonate, 1,5-disulfonate, and 2,6-disulfonate derivatives of 9,10-anthraquinone and of fluorescein dianion. New information is also presented on 1,4-naphthoquinone. For comparison, H-atom-transfer reactions of the anthraquinone triplets with 2-propanol were also studied. The new triplet–anion results, together with many previously reported data, are analyzed in the framework of a simplified Marcus theory by which the activation energy of formation of the pure charge-transfer exciplex, $\Delta G^{\ddagger}$, was calculated and correlated with the rate constant k_q. Plots of $\log k_q$ vs $\Delta G^{\ddagger}$(calcd) for the various systems reveal three groups of roughly linear correlations. The energetically favored interactions (mostly for I^-, N_3^-, SCN^-, and NO_2^- with $\Delta G^{\circ}_{CT} \leq 0.2$ eV) display the theoretical slope $-1/(2.3RT)$. For endoergic interactions, two additional straight lines appear with successively smaller slopes that relate both to the respective magnitudes of ΔG°_{CT} and to specific anion effects. This behavior is interpreted in terms of partial charge transfer in the reaction complex. Our comparative study bears also on the question of $n\pi^*$ vs $\pi\pi^*$ reactivity in charge-transfer interactions. No intrinsic difference in CT reactivity between these two electronic configurations is found either in their quenching kinetics or in the quantum yields of resulting radicals. The reactivity of the organic triplet depends essentially on its thermodynamic properties (reduction potential and triplet energy). That of the anion depends also on specific properties, including its (large) reorganization energy (affecting the quenching kinetics) and spin–orbit coupling within the incipient inorganic radical (affecting the bulk radical yield). For anions that contain H-atom (such as HCO_2^-), the possibility of H-transfer is suggested in some cases. Also discussed, in light of the new results, is the difference in reactivity between 1- and 2-sulfonated derivatives of anthraquinone, representing respectively "weak" and "strong" sensitizers.

Introduction

In the course of extensive laser flash photolysis studies of charge-transfer (CT) quenching of organic triplets by simple anions in aqueous solution, we have recently suggested a kinetic analysis based on classical Marcus theory, in which large reorganization energies are assigned to the anions alone.[1] These energies, which are derived from spectroscopic ($h\nu_{CTTS}$) or photoionization threshold (E_t) measurements, enabled us to calculate the activation free energies, $\Delta G^{\ddagger}$, of the quenching reactions and to correlate them with the rate constants k_q. However, the number of triplets treated in this manner was quite limited. We now present a further treatment of a large number of triplet–anion systems, including new data mostly on 9,10-anthraquinonesulfonates. This extends our previous study of 9,10-anthraquinone-2-sulfonate[1-3] with special attention now focused on 1- and 1,5-sulfonates ("weak" sensitizers) whose electronic configuration ($\pi\pi^*$) is different from that of 2- and 2,6-derivatives ($n\pi^*$, "strong" sensitizers).[4]

The dependence of $\log k_q$ on $\Delta G^{\ddagger}$(calcd) for the numerous and varied systems included in our discussion brings out hitherto unexpected systematic groupings which relate both to the magnitude of free energy change involved in the CT process and to specific anion effects. The reason for this behavior is discussed. In addition, the results bear on the question of whether the well-known difference in reactivity between $n\pi^*$ and $\pi\pi^*$ triplets in their H-abstraction reactions occurs also in charge-transfer interactions. The data for anion quenchers that can *only* function by charge transfer show that in such cases there is no intrinsic difference in reactivity between these two electronic configurations. This applies to their overall reaction patterns, to quenching rates, and to quantum yields of free radicals produced in bulk by the redox reactions.

Experimental Section

Materials and Solutions. Sodium 9,10-anthraquinone-2-sulfonate (AQ2S), 1,4-naphthoquinone (NQ), sodium formate, 2-propanol, and the inorganic materials were of Analar or puriss grades and were used as received. DCO_2K (99% D) was obtained from Aldrich. Acetonitrile (Fluka "Garantie" for UV spectroscopy and Burdick Jackson UV grade) was also used without further purification. The sodium salts of anthraquinone-1-sulfonate (AQ1S) (ICN Pharmaceuticals), anthraquinone-2,6-disulfonate (AQ26DS), and anthraquinone-1,5-disulfonate (AQ15DS) (both Aldrich) were recrystallized at least twice either from ethanol or from water. Fluorescein (Fluka) was chromatographed on activated alumina, precipitated by addition of 0.1 M HCl, and dried at 60 °C. Water was purified by a Millipore-Q system.

Solutions were deaerated or saturated with 1 atm of O_2 by bubbling N_2 or O_2, respectively. Unbuffered solutions were used except in the following cases. (a) Yields of the anion radical $AQ1S^{\bullet-}$ were first measured in 10^{-2} M phosphate buffer (pH 7.5) because the pK of AQ1SH (semiquinone) is 5.4.[5] However, it was realized that the rate of protonation in unbuffered neutral solutions is slow on the time scale of these measurements, and later no buffer was used. (b) Fluorescein was studied

† Hebrew University.
‡ Brandeis University.

(1) Loeff, I.; Treinin, A.; Linschitz, H. *J. Phys. Chem.* **1992**, *96*, 5264.
(2) Loeff, I.; Treinin, A.; Linschitz, H. *J. Phys. Chem.* **1984**, *88*, 4931.
(3) Loeff, I.; Goldstein, S.; Treinin, A.; Linschitz, H. *J. Phys. Chem.* **1991**, *95*, 4423.
(4) Moore, J. N.; Philips, D.; Nakashima, N.; Yoshihara, K. *J. Chem. Soc., Faraday Trans. 2* **1987**, *83*, 1487.

0002-7863/93/1515-8933$04.00/0

in 10^{-2} M NaOH where it is present as its dianion. Its triplet decay was followed at 550 nm, where the ground-state absorption is relatively low.

AQ2S and AQ26DS solutions containing high concentrations of HCO_2^- or 2-propanol gave irreproducible results in O_2-free solutions. Flushing the solutions with O_2 before pulsing solved this difficulty and also prevented the secondary reduction stage.[3]

Apparatus and Procedure. The carbonyl compounds were excited at 337.1 nm by a pulsed nitrogen laser (P.R.A. LN-1000, 0.5 ns, 1.5 mJ). In some cases a Nd:YAG laser (System 2000, JK Lasers) at its third harmonic (354 nm) was used. Kinetic traces were digitized and displayed by either a Tektronix 2440 or a TDS 520 oscilloscope. An Olivetti PC was used for averaging and storing data. The other components were conventional, including a pulsed Xe lamp, a monochromator, and a fast photomultiplier, with collinear measuring and excitation beams.

The concentration of the carbonyl compound was usually adjusted to give absorbance of ~1 at 337 nm, except for experiments with NO_2^-, where a higher absorbance was used. Inner-filter corrections were made when necessary.[1]

Second-order rate constants, k_q, for quenching of triplets were obtained from the linear dependence of pseudo-first-order triplet decay constants on quencher concentration, following the triplet absorption near its peak (about 400 nm for the anthraquinonesulfonates). For AQ1S and AQ15DS, the absence of triplet–water reactions (which lead to overlapping transient absorptions) made these measurements simpler than for AQ2S and AQ26DS. However, difficulties were encountered in determining $k_q \leq 10^7$ M^{-1} s^{-1} for AQ1S and AQ15DS, since high concentrations of weakly quenching anions (Cl^- or HCO_2^-) were required to compete with the fast self-decay of their triplets ($\tau < 150$ ns). Plots of their decay constants vs $[X^-]$ were found to curve up above ~1 M (see, e.g., Figure 4 and comments, below). In such cases, k_q was determined from the initial slope, i.e., up to $[X^-]$ ~1 M.

Quantum yields of reduced species, ϕ_R, were measured using the AQS/2MCl$^-$-actinometer ($\phi_{AQS^{\bullet-}} = 0.51$).[3] Extinction coefficients (M^{-1} cm^{-1}) of the anion radicals of AQ2S and AQ1S were taken as 8200 at their peaks (500 nm),[5] and for $NQ^{\bullet-}$, 12 500 at 390 nm.[3] Extinction coefficients of reduced AQ15DS and AQ26DS were determined by the conventional pulse radiolytic method,[6] using a Varian 7715 linear accelerator and associated equipment, as described earlier.[3] The dosimetric system was 10^{-3} M KSCN saturated with N_2O, taking ϵ(480 nm) of $(SCN)_2^{\bullet-}$ = 7600 M^{-1} cm^{-1}.[7] Semiquinone transient absorbances following pulse radiolysis were measured at 510 nm on argon-purged solutions of the quinones (5×10^{-4} M) containing 0.1 M sodium formate. Under these conditions, all radiolytically produced primary radicals (e^-, OH, H) are converted to CO_2^-, which reduces the quinones. To correct the radical yield in these solutions to that corresponding to the SCN^-–N_2O dosimeter (which measures only e^- and OH radicals), the semiquinone absorbances at 510 nm were decreased by 10%, assuming that $G(e^-) = G(OH) = 2.7$ and $G(H) = 0.6$. The values of ϵ_{510}(M^{-1} cm^{-1}) thus obtained are 7400 (AQ15DS) and 9700 (AQ26DS), both ±5%.

In determining ϕ_R at appropriate wavelengths, it is necessary to take account of overlapping absorptions of the organic and inorganic radicals. This is simple for the anthraquinones, since $(SCN)_2^-$ is the only inorganic radical of those studied here that absorbs around 500 nm. In addition, the semiquinones can be selectively removed by oxygen. For these cases, the residual absorbance of $(SCN)_2^-$ was determined at a suitable time after flashing O_2-saturated solutions and subtracted from the combined absorptions of both radicals in O_2-free solutions. All yields were extrapolated back to zero time. However, the absorption of $NQ^{\bullet-}$ overlaps that of the dihalide anions, X_2^-, and the reaction of $NQ^{\bullet-}$ with O_2 is incomplete ($K_{eq} = 0.21$).[3] For the NQ systems, the contributions of the dianions were therefore calculated from their known absorption coefficients at 390 nm,[7] the wavelength selected for study, on the reasonable assumption that $NQ^{\bullet-}$ and X_2^- radicals are formed in equivalent amounts (see Scheme II, below, in section III of the Results and Discussion).

The one-electron reduction potentials of AQ1S, AQ15DS, and AQ26DS were determined by cyclic voltammetry in deaerated 0.1–0.3 M NaOH solutions (containing also 0.1 M NaCl), where the radical anions are relatively stable. An electrochemical analyzer (BAS 100 B) was employed with Ag/AgCl and SnO_2 as reference and working electrodes, respectively, and with scan rates from 5 to 10 mV/s. The voltammograms obtained under these conditions were quite reversible. (As a check, the reduction potential of AQ2S was also measured, giving E° = –0.380 V (vs NHE), in agreement with that derived by pulse radiolysis.[8]) The values of E° determined by this procedure are –0.44 (AQ1S), –0.50 (AQ15DS), and –0.31 V (AQ26DS). They are quite close to previous results which were obtained by polarography (at pH 12) and recently by cyclic voltammetry in 0.5 M NaOH.[9]

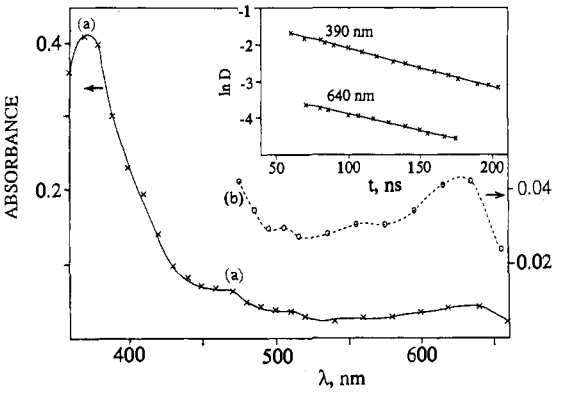

Figure 1. Transient absorption spectrum ~30 ns following laser photolysis of 2×10^{-4} M AQ1S, air-free, pH 7.5. Inset: first-order plots for transient decay at 390 and 640 nm.

Results and Discussion

I. Properties and Reactions of Triplet Anthraquinonesulfonates. A. Triplet Anthraquinone-1-sulfonate (AQ1S). The intermediates produced by laser photolysis ($t \geq 30$ ns) of AQ2S,[10] AQ26DS,[11] and AQ15DS[4] in water have been studied extensively, but apart from a brief remark on its decay kinetics,[12] no such information for triplet AQ1S has been reported. Figure 1 shows the transient absorption produced in aqueous solution of AQ1S at pH 7.5 immediately after the laser flash. It displays an intense band, λ_{max} at 375 nm, and several ill-defined weaker bands at longer wavelengths (ca. 410, 460, and 640 nm). The first-order decay, measured at 380, 390, 450, and 640 nm, is independent of λ (Figure 1, inset), indicating the presence of only one transient species. The rate constant, $k_d^T = (9 \pm 1) \times 10^6$ s^{-1}, of AQ1S is coincidentally close to that of AQ2S in water ($(1.0 \pm 0.2) \times 10^7$ s^{-1}).[10] The spectrum and its sensitivity to oxygen (see below) closely resemble those of the triplets of other sulfonated derivatives of AQ[4] and is therefore assigned to triplet AQ1S. But contrary to the behavior of triplet AQ2S[10] and AQ26DS[11] (the strong sensitizers), whose decay is associated with the formation of longer lived intermediates produced by triplet–water reactions, the AQ1S triplet appears to undergo direct intersystem crossing to the ground state, as noted above. Triplet AQ15DS behaves similarly, and this chemical inertness toward water was considered to be a major characteristic of weak sensitizers.[4] We obtained further evidence for this inertness by studying the effect of steady irradiation at 365 nm on 10^{-3} M AQ1S solution (saturated with 1 atm of O_2); under conditions where AQ2S undergoes efficient photohydroxylation,[10] the AQ1S solution remained unchanged.

The short triplet lifetime of strong sensitizers is due to triplet–water reactions. This is also evidenced by the much slower decay of triplet AQ2S in CH_3CN[10] and even slower decay in Freon.[13]

(5) Hulme, B. E.; Land, E. J.; Phillips, G. O. *J. Chem. Soc., Faraday Trans. 1* **1972**, *68*, 1992.
(6) Schuler, R. H.; Patterson, L. K.; Janata, E. *J. Phys. Chem.* **1980**, *84*, 2088.
(7) Hug, G. L. National Standard Reference Data Series 69 (NSRDS-NBS69); U.S. National Bureau of Standards; U.S. Government Printing Office: Washington, DC, 1981.
(8) For a critical review and compilation of standard one-electron reduction potentials, see: Wardman, P. *J. Phys. Chem. Ref. Data* **1989**, *18*, 1637.
(9) Furman, N. H.; Stone, K. G. *J. Am. Chem. Soc.* **1948**, *70*, 3055. Ranjith, S. K. A.; Gamage, A.; McQuillan, J.; Peake, B. M. *J. Chem. Soc., Faraday Trans.* **1991**, *87*, 3653.
(10) Loeff, I.; Treinin, A.; Linschitz, H. *J. Phys. Chem.* **1983**, *87*, 2536.
(11) Moore, J. N.; Philips, D.; Nakashima, N.; Yoshihara, K. *J. Chem. Soc., Faraday Trans. 2* **1986**, *82*, 745.
(12) Hulme, B. E.; Land, E. J.; Phillips, G. O. *J. Chem. Soc., Faraday Trans. 1* **1972**, *68*, 2003.
(13) Carlson, S. A.; Hercules, D. M. *J. Am. Chem. Soc.* **1970**, *92*, 5611.

On the other hand, we have found that the lifetime of triplet AQ1S in CH_3CN ($k_d^T \sim 10^8$ s^{-1}) is shorter than that in water.[14]

In the absence of triplet–water reactions, the fast decay of triplet weak sensitizers appears to be mainly due to a "special nonradiative process",[15] which is also reflected in low phosphorescence quantum yields[4] (see below). Similar behavior was also observed with other α-substituted anthraquinones (chloro, bromo, and *tert*-butyl substituents) and was attributed to distortion of the planar molecules caused by interaction of the carbonyl group with the α-substituent, which gives rise also to broad phosphorescence spectra.[15,16]

Triplet AQ1S is quenched by O_2 with rate constant $k_q(O_2) \sim 1 \times 10^9$ M^{-1} s^{-1}, as estimated from the lifetime in water equilibrated with 1 atm of O_2 (1.3×10^{-3} M). It is interesting to note that quenching by O_2 is somewhat slower than diffusion-controlled for both strong and weak sensitizers.[4] This may be related to a statistical factor (1/9) if quenching occurs via formation of singlet oxygen. An attempt to measure the rate of self-quenching (^{3}AQ1S* + AQ1S) gave only an upper limit ($k \leq 4 \times 10^8$ M^{-1} s^{-1}) because [AQ1S] could not be raised above 3×10^{-3} M owing to restrictions imposed by absorption of the laser beam at 337 nm. Self-quenching appears to be the only reaction which is faster for the weak compared to the strong sensitizers.[4]

The properties of the lowest-energy triplet of AQ1S closely resemble those of AQ15DS, and accordingly AQ1S is also assigned to $\pi\pi^*$ electronic configuration.[4]

B. Redox Properties of the Triplet Anthraquinonesulfonates. In our study of triplet–anion interactions, we require the reduction potentials of the anthraquinone triplets, $E°(M/M^-) + E_T(M)$, where $E°(M/M^-)$ is the standard one-electron reduction potential of the ground state and $E_T(M)$ is the triplet energy. $E°$ was determined as described (see Experimental Section), but we encountered difficulty in obtaining E_T of the weak sensitizers. The phosphorescence of AQ2S and AQ26DS (strong sensitizers) in CH_3CN and other media is strong enough to allow determination of their 0,0 bands, i.e., their triplet energies E_T.[4,10] This is not the case with the weak sensitizers,[4] as shown also by our unsuccessful attempts to measure the emission spectra of AQ1S in water and in CH_3CN. From the very weak and ill-defined phosphorescence of AQ15DS, its origin was estimated to lie close to that of AQ2S and AQ26DS, around 460 nm.[4] A different conclusion can be reached from a previous study of the phosphorescence spectra of chloroanthraquinones.[16] In EPA and trifluoroethanol (both at 77 K), the 0,0 bands of AQ and AQ2Cl are close to 450 nm while those of AQ1Cl and AQ15DCl are shifted to 510 nm (505 nm for crystalline AQ1Cl at 4 K). Moreover, the phosphorescence spectrum of AQ1S was reported to be very similar to that of AQ1Cl.[17] We thus conclude that the E_T values of AQ1S and AQ15DS are lower by ~0.32 eV than that of AQ2S, i.e., 2.36 eV. This conclusion is in accord with our observation that the $k_q(NO_2^-)$ values of these triplets are lower than diffusion-controlled. Judging from the values of $k_q(NO_2^-)$ of aromatic hydrocarbons,[18] k_q should be diffusion-controlled for triplets with $E_T \geq 2.5$ eV, corresponding to efficient energy transfer to NO_2^-,[1,18] and decrease to about 4×10^8 M^{-1} s^{-1} at $E_T \sim 2.35$ eV (e.g., coronene and fluoranthene). Moreover, as shown below, charge-transfer quenching rather than energy transfer may be the main contributor to $k_q(NO_2^-)$ of these weak sensitizers because of their highly negative $\Delta G°_{CT}$. Considering both $E°$ and E_T (summarized in Table I), it is evident that the weak sensitizers are weaker oxidizers than the strong ones and that this *partly* accounts for their weakness (see below).

C. Interaction of Triplet Anthraquinonesulfonates with 2-Propanol. For comparison with pure electron transfer, as exemplified in quenching by anions, we also studied interactions of the quinone triplets with an H-donor, 2-propanol. Quenching constants were measured, and the values obtained for k_q are AQ26DS, 5.9×10^7; AQ2S, 1.0×10^7; AQ1S, 2.8×10^6; and AQ15DS, 1.7×10^6 (M^{-1} s^{-1}) (AQ itself in benzene,[12] 2.1×10^7 M^{-1} s^{-1}). These rate constants are rather high relative to other H-atom transfers, and there is no abrupt change in going from $^3n\pi^*$ (AQ26DS and AQ2S) to $^3\pi\pi^*$ (AQ1S and AQ15DS); in fact, log k_q increases almost linearly with triplet reduction potential $E° + E_T$,[19] suggesting a corresponding charge-transfer contribution to the reaction complex.[20] The high reactivity of quinones compared with ketones, for both $n\pi^*$ and $\pi\pi^*$ states (first observed with chloroanthraquinones in ethanol[21]), was explained on the basis of the tunnel effect theory as due to smaller coordinate displacement and hence smaller barrier width for H-abstraction.[22] The drop in reactivity along the series of α-chloroanthraquinones in ethanol (AQ1Cl > AQ15DCl > AQ18DCl) was attributed to the mixed $\pi\pi^*$–$n\pi^*$ character of the lowest triplet owing to the close proximity of these levels and the gradual increase in the $\pi\pi^*$ contribution.[21]

Contrary to the absence of sharp discontinuity in quenching kinetics, there is an abrupt drop in chemical effect (quantum yield of semiquinone corrected for fractional quenching) on going from $^3n\pi^*$ to $^3\pi\pi^*$. Quantum yields close to 1 were measured for AQ2S and AQ26DS (in O_2-saturated solutions; see Experimental Section), whereas those for the weak sensitizers were found to be close to 0. Thus, it appears that the main reason for the weakness of the weak sensitizers is efficient deactivation within the reaction complex. The fate of the complex is determined by competition between two processes, radical separation and deactivation, with relative rates depending on specific molecular parameters (not necessarily reflecting thermodynamic properties) such as spin–orbit (SO) coupling or the rate of proton transfer. The former effect is responsible for very low radical yields in parallel with fast quenching of triplets by halide ions.[2] In the cases considered here, a possible charge-transfer interaction involving the alcohol p-orbital lone pairs and a $\pi\pi^*$ system, in an appropriate configuration, might lead to a larger SO coupling than a similar interaction with an $n\pi^*$ system and thus cause faster deactivation in the $\pi\pi^*$ complex.[23] Moreover, the greater degree of charge transfer in the alcohol–$n\pi^*$ complex compared to the $\pi\pi^*$ case, as indicated by their relative quenching rates, may also result in faster proton transfer, corresponding to the enhanced acidity and basicity of the incipient proton donor and acceptor components of the $n\pi^*$ complex.[3] Finally, the inertness of the weak sensitizers may be due not to their $\pi\pi^*$ configuration but to interaction of the closely situated carbonyl and 1-sulfonate groups, an interaction which requires a smaller and stronger electron donor (such as HCO_2^-; see below, section III) in order to obtain access for hydrogen transfer.

II. Triplet–Anion Interactions. A. Quenching Rate Constants: Dependence on $\Delta G^‡$. Table I summarizes the new results together with extensive data on other systems in aqueous or water-rich solutions (for sources, see footnotes to Table I). The organic triplets covered here include both $n\pi^*$ states (e.g., AQ2S,

(14) Following triplet decay, the kinetic trace shows a fast buildup of a second intermediate, which then decays with $k_d \sim 10^7$ s^{-1}. AQ15DS acts similarly. This behavior suggests that triplets of the weak sensitizers react with acetonitrile, possibly by formation of an adduct.

(15) Hamanoue, K.; Nakayama, T.; Kajiwara, Y.; Yamaguchi, T.; Teranishi, H. *J. Chem. Phys.* **1987**, *86*, 6654.

(16) Hamanoue, K.; Nakayama, T.; Ito, M. *J. Chem. Soc., Faraday Trans.* **1991**, *87*, 3487.

(17) Kuboyama, A.; Matsuzaki, S. Y. *Symposium on Molecular Structure and Electronic State*; Sendai, Japan, **1983**; p 88 (reported in ref 15).

(18) Treinin, A.; Hayon, E. *J. Am. Chem. Soc.* **1976**, *98*, 3884.

(19) The plot of log k_q vs $E° + E_T$ shows marked but random deviations from linearity. The data can be roughly fitted to a straight line with slope ~2 eV^{-1}.

(20) Cohen, S. G.; Parola, A.; Parsons, G. H. *Chem. Rev.* **1973**, *73*, 141.

(21) Hamanoue, K.; Nakayama, T.; Tanaka, A.; Kajiwara, Y.; Teranishi, H. *J. Photochem.* **1986**, *34*, 73.

(22) Formosinho, S. J. J. Chem. Soc., Faraday Trans. 2 **1976**, *72*, 1332. Formosinho, S. J.; Arnaut, L. G. *Adv. Photochem.* **1991**, *16*, 67.

(23) Okada, T.; Karaki, I.; Matsuzawa, E.; Mataga, N.; Sakata, Y.; Misumi, S. *J. Phys. Chem.* **1981**, *85*, 3957.

Table I. Quenching Constants (log k_q) and Charge-Transfer Free Energies ($\Delta G°_{CT}$, eV) for Triplet–Anion Interactions[a]

triplet[b]	I^-	N_3^-	SCN^-	Br^-	OH^-	Cl^-	NO_2^-	HCO_2^- [c]	$-E°(M/M^-)$,[d] V(NHE)	E_T, eV
1. duroquinone($n\pi^*$)[e]	9.95			9.60	9.18	7.00			0.26[f]	2.40
	−0.81			−0.22	−0.23	0.36				
2. 1,4-naphthoquinone($n\pi^*$)[g]	9.92	9.62	9.78	9.89		9.23	9.70	9.48[h]	0.12	2.48
	−1.03	−1.01	−0.70	−0.44		0.14	−1.32			
3. AQ2S($n\pi^*$)[i]	9.62	9.49	9.59	9.58	8.48	8.97	9.50	8.60[h]	0.38	2.68
	−0.97	−0.95	−0.64	−0.38	−0.39	0.20	−1.26	(8.54)[h]		
4. AQ26DS($n\pi^*$)[j]					8.48	~8.9	9.15[k]	8.52	0.31	2.68
					−0.46	0.13	−1.33			
5. AQ1S(π,π^*)[j]	9.56	9.34	9.50	8.82		6.18	9.00	6.40[g]	0.45	2.36
	−0.58	−0.56	−0.25	0.01		0.59	−0.87	(6.08)		
6. AQ15DS(π,π^*)[j]		9.08	9.15	8.45	~7.1[k]	5.84	8.52	6.60	0.50	2.36
		−0.51	−0.20	0.06	0.05	0.64	−0.82	(5.81)		
7. acetone($n\pi^*$)[l]	9.85	8.54	9.30	6.74			9.48		2.1	3.4
	0.03	0.05	0.36	0.62			−0.3			
8. biacetyl($n\pi^*$)[m]	9.74		9.23	7.75		3.08			0.66	2.48
	−0.49		−0.16	0.10		0.68				
9. benzophenone($n\pi^*$)[n]	9.54	9.11	9.32	7.70	6.69	5.34			1.20	2.99
	−0.46	−0.44	−0.13	0.13	0.12	0.71				
10. benzophenone-4-carboxylate($n\pi^*$)[o]	9.36	9.32	9.34	8.70	7.00	4.90	9.48	7.11[h]	1.13	2.96
	−0.50	−0.48	−0.17	0.09	0.08	0.67	~0.79	(6.93)[h]		
11. *p*-methoxybenzophenone(n,π^*)[n]	9.41	9.52	8.11	6.86	6.00	5.98			1.28	2.99
	−0.38	−0.36	−0.05	0.21	0.20	0.79				
12. benzaldehyde(n,π^*)[n]						6.00			1.27	3.10
						0.67				
13. acetophenone($n\pi^*$)[n]	9.36	9.54	9.34	7.04	6.11	5.70			1.58	3.21
	−0.30	−0.28	0.03	0.29	0.28	0.87				
14. *p*-methoxyacetophenone($\pi\pi^*$?)[n]	9.30	10.08	8.00	6.69	5.51	4.20			1.43	3.14
	−0.38	−0.36	−0.05	0.21	0.20	0.79				
15. 1-naphthaldehyde($\pi\pi^*$)[p]	8.45	7.38					9.20		1.11	2.45
	−0.01	0.01					−0.30			
16. 1-acetonaphthone($\pi\pi^*$)[p]	6.57	5.30					9.38		1.26	2.52
	0.07	0.09					−0.22			
17. 2-acetonaphthone($\pi\pi^*$)[p]	7.15	6.08	4.18	4.30			9.50		1.25	2.59
	−0.01	0.01	0.32	0.58			−0.30			
18. xanthone($\pi\pi^*$)[q]	9.85	9.69	9.78	7.41			9.75		1.40	3.21
	−0.48	−0.46	−0.15	0.11			−0.77			
19. 2-nitrothiophene($\pi\pi^*$)[r]	9.93		9.94	9.90	9.18	7.94			0.39	2.57
	−0.85		−0.52	−0.26	−0.27	0.32				
20. 3-benzoylpyridine($n\pi^*$)[m]	9.79		9.71	9.29		5.63			0.94	2.89
	−0.62		−0.29	−0.03		0.55				
21. eosin($\pi\pi^*$)[s]	7.08	6.20	4.08				5.95		0.61	1.86
	0.08	0.10	0.41				−0.21			
22. fluorescein($\pi\pi^*$)[t]	6.68	4.36					4.83		0.95	2.05
	0.23	0.25					−0.06			
23. 3-methyllumiflavin($\pi\pi^*$)[u]		9.63					9.18		0.49	2.17
		−0.33					−0.64			
24. thionine($\pi\pi^*$)[u]		8.26					6.83		0.25	1.70
		−0.10					−0.41			
25. thiopyronine($\pi\pi^*$)[u]		4.85					6.70		0.43	1.80
		−0.02					−0.33			
$E°(X/X^-)$,V(NHE)[v]	1.33	1.35	1.66	1.92	1.91	2.50	1.04			
$\bar{R}$, eV[w]	1.52	1.57	1.45	1.75	2.06	1.98	2.24			

[a] $\Delta G°_{CT}$ was evaluated by means of the Rehm–Weller equation, ignoring the electrostatic interaction term (see text). Its values are recorded below those of log k_q. Only systems in aqueous or water-rich solutions (neutral unless otherwise stated) are included. [b] The electronic configuration of the triplet (in parentheses) may be "mixed" in some cases. [c] Data for $\Delta G°_{CT}$ are not given since $E°(HCO_2/HCO_2^-)$ is not known; it should be considerably higher than $E°(COOH/HCO_2^-) = 1.55$ V (ref 3). In parentheses, log k_q for DCO_2^- in D_2O. [d] In some cases it is not certain whether $E°$ corresponds to a single one-electron reduction process or to an average of two such reductions. [e] Scaiano, J. C.; Neta, P. *J. Am. Chem. Soc.* **1980**, *102*, 1608. 4:1(v/v) H_2O/CH_3OH. The order $n\pi^*$ vs $\pi\pi^*$ may depend on solvent polarity, with the latter being lower in polar solvents (Amouyal, E.; Bensasson, R. *J. Chem. Soc., Faraday Trans. 1* **1976**, *72*, 1274). [f] Reference 8. [g] Reference 1 and present work. [h] Reference 3. [i] Reference 2. A revised value for $k_q(Cl^-)$ is reported here. [j] Present work. For $E°$ and E_T, see text. [k] Reference 4. [l] Reference 1 and 18. The exceptionally high value for $k_q(SCN^-)$ may be due to the energy-transfer mechanism. [m] Massetti, F.; Mazzucato, U. *Gazz. Chim. Ital.* **1979**, *109*, 557. [n] Shizuka, H.; Obuchi, H. *J. Phys. Chem.* **1982**, *86*, 1297. 4:1(v/v)H_2O/CH_3CN. [o] Reference 38. pH 11.2. [p] Reference 18. In some cases, 1–5% 1,1-dimethylethanol was added. [q] Present work and reference 1. pH 12; 16%(v/v)CH_3CN; $E°$ and E_T from Abdullah, K. A.; Kemp, T. J. *J. Chem. Soc., Perkin Trans. 2* **1985**, 1279. The order of $n\pi^*$ vs $\pi\pi^*$ may depend on solvent polarity, with the latter being lower in polar solvents (Garner, A.; Wilkinson, F. *J. Chem. Soc., Faraday Trans. 2* **1976**, *72*, 1010). [r] Martins, L. J. *J. Chem. Soc., Faraday Trans. 1* **1982**, *78*, 519, 533. In nonpolar solvents, an $n\pi^*$ level was considered to be lower. [s] Reference 1. pH 9.1; $E°$ from reference 24. [t] Present work. pH 12; $E°$ from Compton, R. G.; Coles, B. A.; Pilkington, M. B. G. *J. Chem. Soc., Faraday Trans. 1* **1988**, *84*, 4347. E_T from Engel, P. S.; Monroe, B. M. *Adv. Photochem.* **1971**, *8*, 245 (Table XII). [u] Winter, G.; Shioyama, H.; Steiner, U. *Chem. Phys. Lett.* **1981**, *81*, 547. [v] Reference 8. [w] Reference 1.

AQ26DS, 1,4-naphthoquinone, acetone, benzaldehyde, and derivatives of benzophenone) and $\pi\pi^*$ states (e.g., AQ1S, AQ15DS, naphthyl carbonyls, and class I dyes[24]). In some cases (like the acetophenones), state-switching may occur in water, lowering the $\pi\pi^*$ level below the $n\pi^*$ level.[25] Table I also includes data on standard free energies of the CT process $^3M + X^- \rightarrow M^- +$

(24) Grossweiner, L. J.; Kepka, A. G. *Photochem. Photobiol.* **1972**, *16*, 305.

(25) Turro, N. J. *Modern Molecular Photochemistry*; Benjamin/Cummings: Menlo Park, CA, 1978; Chapter 10.

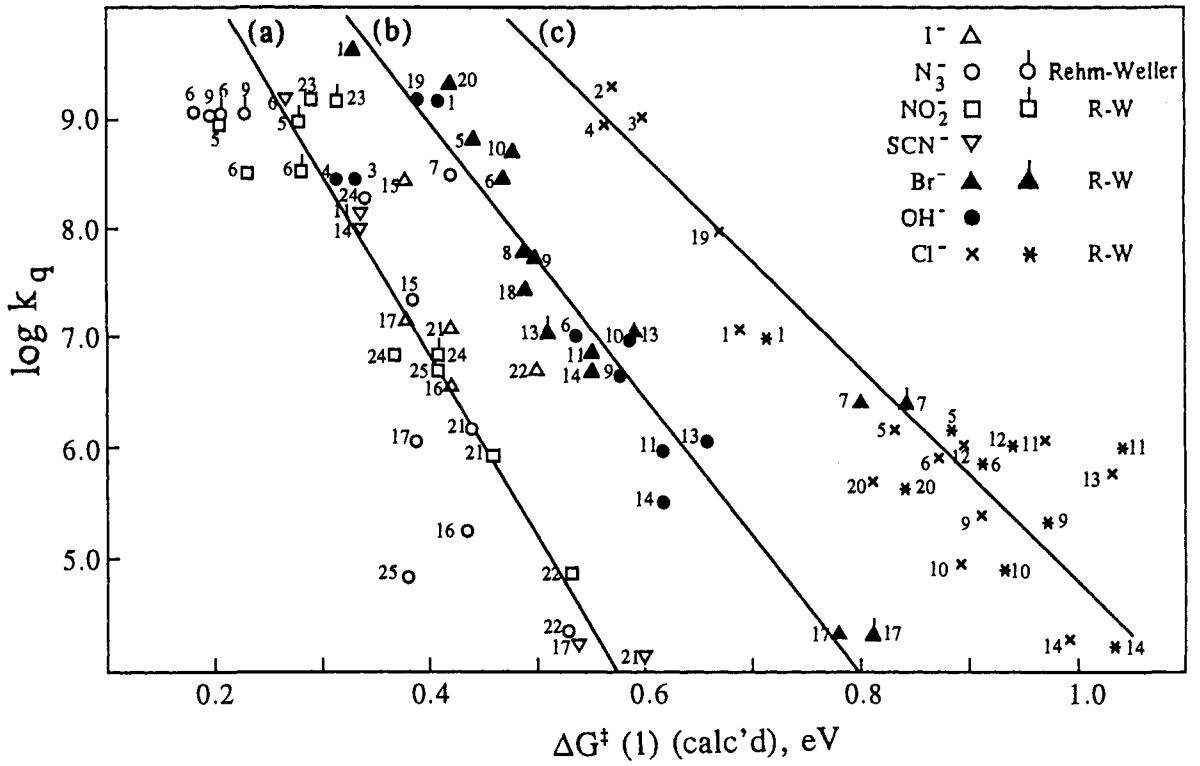

Figure 2. Kinetics of triplet–anion interactions. Dependence of quenching rate constant on the calculated free energy of activation (see text). For the numbers used to designate the organic triplets, see Table I.

X, calculated by means of the equation[26] $\Delta G°_{CT} = E°(X/X^-) - [E°(M/M^-) + E_T(M)]$, where $E°(X/X^-)$ and $E°(M/M^-)$ are standard reduction potentials of the corresponding couples and $E_T(M)$ is the triplet energy of the organic molecule (all given in Table I). The electrostatic interaction term is neglected; it is either zero for uncharged M and mononegative anion quencher or relatively small because of the high dielectric constant of water.

Consider the familiar Rehm–Weller scheme,[26] as applied to these systems:

Scheme I

$$^3M^* + X^- \underset{k_{-1}}{\overset{k_1}{\rightleftharpoons}} (^3M^*\cdot X^-) \underset{k_{-2}}{\overset{k_2}{\rightleftharpoons}} {}^3(M^-\cdot X)$$
$$\downarrow k_0 \qquad\qquad\qquad\qquad \downarrow k_3$$

where k_3 is the combined rate constant for intersystem crossing (leading to deactivation) and dissociation to free radicals: $k_3 = k_{ISC} + k_{fr}$. When $k_2 \ll k_{-1}$, this yields

$$k_q = K_d k_2 (1 + k_{-2}/k_3)^{-1} \quad (1)$$

where $K_d = k_1/k_{-1}$ is the diffusional equilibrium constant. Assuming also that $k_{-2} \ll k_3$ (see below), eq 1 reduces to that for the activation-controlled case:

$$k_q = K_d k_2 = \nu \exp(-\Delta G^{\ddagger}/RT) \quad (2)$$

where $\Delta G^{\ddagger}$ is the free energy of activation for the forward electron transfer leading to the equilibrated pure charge-transfer exciplex $^3(M^-\cdot X)$, and ν, which incorporates the equilibrium constant, K_d, has dimensions $M^{-1}\,s^{-1}$. However, since $K_d \sim 1\ M^{-1}$ (see below), ν is numerically close to the frequency of electron transfer within the pair (ranging from 10^{12} to $10^{14}\ s^{-1}$ [27]). $\Delta G^{\ddagger}$ is obtained for these anionic systems by a simplified application of the Marcus equation, in which the total reorganization energy λ is replaced by the intrinsic reorganization energy $\bar{R}$ of the relatively small inorganic anions:[1]

$$\Delta G^{\ddagger}_M = (\bar{R}/4)(1 + \Delta G°_{CT}/\bar{R})^2 \quad (3)$$

(for the values of $\bar{R}$ used here, see Table I). $\Delta G^{\ddagger}$ was also calculated by means of the empirical Rehm–Weller equation[26] similarly simplified by replacing λ by $\bar{R}$:

$$\Delta G^{\ddagger}_{RW} = [(\Delta G°_{CT}/2)^2 + (\bar{R}/4)^2]^{1/2} + \Delta G°_{CT}/2 \quad (4)$$

In most cases the two equations gave values agreeing within 0.02 eV. Figure 2 presents the dependence of log k_q on $\Delta G^{\ddagger}$(calcd) for those systems where quenching is considerably slower than diffusion-controlled. (When $\Delta G^{\ddagger}_M$ and $\Delta G^{\ddagger}_{RW}$ differ appreciably, the system is represented by two points.)

B. Grouping of Quenching Reactions: Charge Transfer in the Reaction Intermediate. According to Figure 2, the systems appear to fall into three groups, with different linear correlations between log k_q and $\Delta G^{\ddagger}$. For systems with relatively low reaction free energies ($\Delta G°_{CT} \lesssim 0.2$ eV), the line designated (a) has slope $-16.5 \pm 1\ eV^{-1}$, agreeing within experimental uncertainty with the theoretical value $-(2.3RT)^{-1} = -16.9\ eV^{-1}$. These cases comprise the more oxidizable anions (I^-, N_3^-, SCN^-, and NO_2^-) and a few OH^- systems. This strongly supports the assumptions made in applying spectroscopically derived anion reorganization energies and classical Marcus theory to the triplet quenching situation.[1] The fact that the weak sensitizer–NO_2^- systems also fall on this line supports our view that electron-transfer quenching in these cases predominates over possible energy transfer, as noted earlier (section IB).

Endoergic CT interactions tend to display marked deviations from the theoretical line, but they can still be grouped around two lines which relate both to the magnitude of $\Delta G°_{CT}$ involved and to specific anion effects. Line (b) represents the Br^- and OH^- systems with $\Delta G°_{CT}$ in the range 0.1–0.4 eV. The still more endoergic Cl^- systems (and also acetone/Br^- with $\Delta G°_{CT} = 0.62$ eV) fall on line (c). The slope (absolute value) decreases stepwise from line (a) to line (c): ~16, ~12, and ~10 eV^{-1}, respectively. Within considerable uncertainty (the Cl^- points scatter rather

(26) Rehm, D.; Weller, A. *Isr. J. Chem.* **1970**, *8*, 259.
(27) Sutin, N. *Acc. Chem. Res.* **1982**, *15*, 275.

widely around the straight line), the intercepts display an opposite trend, increasing from about 13.5 for (a) to roughly 14.5 for (c).[28]

It should be noted here that the approximation $k_{-2} \ll k_3$ becomes less justified as the activation energy of the reverse electron transfer, $\Delta G^{\ddagger}_{-2} = \Delta G^{\ddagger} - \Delta G^{\circ}_{CT}$, decreases. In Figure 2, we should actually plot $\log[k_q(1 + k_{-2}/k_3)]$ against $\Delta G^{\ddagger}$ (see eqs 1 and 2) if reliable values for k_{-2} and k_3 were known. However, a rough estimate shows that for most of the triplet–anion systems, with $\Delta G^{\ddagger} - \Delta G^{\circ}_{CT} \gtrsim 0.3$ eV, the correction term $\log(1 + k_{-2}/k_3)$ can be neglected. Thus, with $k_{-2} = \nu_{-2} \exp[-(\Delta G^{\ddagger} - \Delta G^{\circ}_{CT})/RT]$, and taking $\nu_{-2} \sim \nu_2 \sim 10^{13}$ s^{-1} and $k_3 = k_{ISC} + k_{fr} \gtrsim 10^9$ s^{-1} (since no exciplexes could be detected, see also ref 2), we obtain $k_{-2}/k_3 \lesssim 0.1$ for $\Delta G^{\ddagger} - \Delta G^{\circ}_{CT} \gtrsim 0.3$ eV. While the correction may be significant for a few of the Cl^- and other systems with $\Delta G^{\ddagger} - \Delta G^{\circ}_{CT} \lesssim 0.2$ eV, the essential features of Figure 2 should not be changed by including the effect of reverse electron transfer. Indeed, it would be particularly interesting to focus attention directly on the rates of formation of the complex, as measured by Kk_2 in Scheme I. Differences in these rates and associated groupings would be even more marked than those of Figure 2 if corrections were made for k_{-2} (increasing with increasing ΔG°_{CT}) in calculating Kk_2 from the measured k_q's (eq 1).

In an attempt to interpret the role of free energy, ΔG°_{CT}, in these groupings, let us consider the nature of the rate-determining electron-transfer reaction, which is usually expressed by the equation:

$$(^3M^*\cdot X^-) \rightarrow {}^3(M^-\cdot X)$$

where $(^3M^*\cdot X^-)$ is the encounter pair and $^3(M^-\cdot X)$ is the "pure" equilibrated CT exciplex. This equation corresponds to complete transfer of an electron from anion to triplet, and on its basis, the energy terms, required to calculate $\Delta G^{\ddagger}$ (eq 3), were obtained. Thus, the Rehm–Weller equation for ΔG°_{CT} clearly corresponds to transfer of one electron from X^- to $^3M^*$ (all species equilibrated), and the values of $\bar{R}$, derived from electron-detachment spectra, correspond to vertical removal of one electron from the anion either to vacuum (E_t) or to solvent ($h\nu_{CTTS}$).[1]

Now, as the electron transfer becomes more and more endoergic, *partial* charge transfer should be considered, in which the exciplex is better represented as $^3(M^{-\Delta e}\, X^{-(1-\Delta e)})$, with $\Delta e \leq 1$. If we may discuss the electron transfer in terms of an outer-sphere mechanism even when $\Delta e < 1$ (that is, if the transition state is only weakly bonded, see below), then we should modify eq 3 (which applies to outer-sphere interactions) by considering the effect of $\Delta e < 1$ on ΔG°_{CT} and $\bar{R}$. Assuming that these quantities are proportional to Δe and $(\Delta e)^2$, respectively,[29] we obtain

$$\Delta G^{\ddagger} = (\Delta e)^2(\bar{R}(1)/4)[1 + \Delta G^{\circ}_{CT}(1)/(\Delta e)\bar{R}(1)]^2 \sim (\Delta e)^2 \Delta G^{\ddagger}(1) \quad (5)$$

where (1) stands for $\Delta e = 1$. As an approximation we put $\Delta e = 1$ in the $\Delta G^{\circ}/\bar{R}$ term, which is appreciably smaller than 1 for most of our systems. (Even for $\Delta e = 0.7$, see below, the error introduced is less than 25% in most cases.) Equations 2 and 5 lead to a modified correlation between $\log k_q$ and the *calculated* values of $\Delta G^{\ddagger}(1)$:

$$\log k_q = \log \nu - [(\Delta e)^2/2.3RT]\Delta G^{\ddagger}(1) \quad (6)$$

Thus, the slopes of the lines shown in Figure 2 should be $-(\Delta e)^2/(2.3RT)$, reaching the value -16.9 eV^{-1} only when $\Delta e = 1$ (line (a)). From the other two lines we can estimate the average charge transferred to be $\sim$0.85 e and $\sim$0.77 e for groups (b) and (c), respectively. Moreover, the striking increase in anion quenching rate in passing from group (a) to group (c), for given values of the *calculated* $\Delta G^{\ddagger}(1)$, would thus correspond, to a large extent, to decreasing magnitudes of the *actual* reorganization energies in forming the exciplex, in parallel with decreasing values of Δe.

It should be emphasized that eq 6 is applicable only when ΔG°_{CT} is much smaller than the reorganization energy, which is the case for the triplet–anion systems (large $\bar{R}$). When the situation is reversed, $\Delta G^{\ddagger}$ and ΔG°_{CT} nearly coincide (as clearly seen from eq 4), and if ΔG°_{CT} is still proportional to Δe, then we expect a linear correlation between $\log k_q$ and ΔG°_{CT} with slope $-(\Delta e)/(2.3RT)$. Such (or similar) correlations were obtained for several organic systems and were also interpreted on the basis of partial charge transfer. For example, *two* straight lines were obtained for $\log k_q$ of triplet benzophenone on plotting against the ionization potentials of 17 donors. Their slopes are small but different for aliphatic and aromatic quenchers, respectively.[20] This also may be the case with the 2-propanol–anthraquinone-sulfonates (section IC).[19] However, we should be careful in deriving Δe from the slopes of such lines because (a) ΔG°_{CT} may not be proportional to Δe when it is small and (b) with organic quenchers, proton transfer may be involved in the reaction coordinate without any minimum in the potential surface which corresponds to a definite CT exciplex.

There is, however, a further large question raised by Figure 2: Why do the systems divide into *separate* groups, with some of them (like 2-acetonaphthone with SCN^- and Br^-; NQ, AQ2S, and AQ26DS with Cl^-) grouped not according to the magnitude of ΔG°_{CT} but to the anion involved? The group separations and associated intercepts are evidently directly dependent on the values taken for the one-electron redox potentials listed in Table I, which represent averages of the best data available.[8] However, the effects of uncertainties in these potentials on the groupings of Figure 2 are slight, particularly since $\Delta G^{\circ}_{CT}/\bar{R}$ is relatively small for these inorganic systems. Apparently there is some specific effect of the anion, whose nature is not clear, superimposed on that of ΔG°_{CT}; perhaps some oversimplification in our calculation of $\Delta G^{\ddagger}$ is indicated. Nevertheless, the consistency and regularity of the grouping support its validity. For possible approaches to this problem, let us consider the origin of $\Delta e < 1$ and the frequency factor ν.

Partial charge transfer can be viewed as back electron transfer or a charge shift within the exciplex $^3(M^-\cdot X)$ from M^- to X. Such a shift may correspond to a complex structure analogous to that involved in the much studied halogen atom complexes with many organic and inorganic electron donors.[31] The difference is that in the CT exciplex both species are radicals with parallel spins, and we may consider that when a paired electron of M^- is removed,

(28) It is interesting that the quite well-defined groupings in Figure 2 become much less marked when $\log k_q$ is plotted directly against ΔG°_{CT}, with no consideration of reorganization energy. The points are scattered over a wide region lying between those for NO_2^- (lowest quenching rates) and Cl^- (highest rates). At $\log k_q = 7$, the values of ΔG°_{CT} for the two extreme cases, NO_2^- and Cl^-, are about -0.4 and 0.4 V with slopes approximately -6.3 and -7.0 eV^{-1}, respectively. In this connection, we note that the reorganization energy of NO_2^- (2.24 eV) contains also a large inner component (0.77 eV),[1] which is not present for the other anions. When this is taken into account, using the *total* value of $\bar{R}$ for all cases, the NO_2^- points group closely with the other anions on line (a) of Figure 2.

(29) The assumption that ΔG°_{CT} is proportional to Δe seems to be a good approximation as long as Δe is close to 1, which is the case with the systems examined here (see text). As for the reorganization energy, we have to consider outer- and innersphere contributions. The former, λ_{out}, is given by the Marcus equation, $\lambda_{out} = (\Delta e)^2(1/2r_D + 1/2r_A - 1/r_{AD})(1/\epsilon_{op} - 1/\epsilon_s)$, where Δe is the charge transferred in the electron-transfer reaction.[30c] (Usually Δe is taken as 1 without due consideration of the real nature of charge distribution in the product of this elementary reaction.) The dependence of the inner-sphere contribution λ_i on Δe is more complicated since it involves specific structural changes in the reacting species. Still, from the Marcus equation, it is clear that the free energy of activation, $\Delta G^{\ddagger}$, is derived from the free energy of reorganization, λ, by multiplying λ by the factor $(\Delta e^{\ddagger}/\Delta e)^2 = {}^1/_4(1 + \Delta G^{\circ}_{CT}/\lambda)^2$, that is, by the *square* of the fraction of charge transferred in forming the activated complex from its reactants, en route to the final product of the elementary charge-transfer reaction.[30c]

(30) (a) Marcus, R. A. *Annu. Rev. Phys. Chem.* **1964**, *15*, 155. (b) Eberson, L. *Adv. Phys. Org. Chem.* **1982**, *18*, 79. (c) Sutin, N. *Prog. Inorg. Chem.* **1983**, *30*, 441.

(31) (a) Bühler, R. E. *J. Phys. Chem.* **1972**, *76*, 3220. (b) Treinin, A.; Hayon, E. *J. Am. Chem. Soc.* **1975**, *97*, 1716.

M is left in a triplet state. The net effect may be viewed as a resonance between $^3(M^-\cdot X)$ and $(^3M^*\cdot X^-)$, with the latter contribution increasing with increasing electron affinity of X. We emphasize that the intermediacy of such a resonance hybrid must be clearly distinguished from a situation involving two opposing electron-transfer reactions, as in Scheme I above. It is interesting to note that plots of $h\nu_{max}$ for halogen atom complexes against the ionization potentials of various donors were found to give three straight lines with slopes following the order I > Br > Cl. This result was explained on the basis of a simple resonance theory.[31a] But more important for our discussion is the realization that such resonance imparts an inner-sphere character to the CT interaction. This should cause the kinetics to deviate from the Marcus equation as used here, and therefore values of $\Delta G^{\ddagger}$ calculated by its means become questionable. Thus, only for systems lying on line (a) of Figure 2, with the theoretical slope, can this treatment be safely employed. The deviations shown by lines (b) and (c) may simply reflect the inapplicability of an outer-sphere theory to the actual situation. In any case, the empirical demonstration of different groupings in Figure 2 is still valid, whatever may be its cause.

The frequency factor ν is actually the product of three quantities:[30] the electronic factor κ_{el}; the diffusional equilibrium constant K_d for formation of the encounter pair; and an effective nuclear frequency ν_n (the frequency of passage across the barrier). K_d is close to 1,[32] and κ_{el} attains its maximum value of 1 when the electronic coupling is sufficiently large. The very high frequency factors (around 10^{14} s^{-1}) that we obtained can perhaps be explained by assuming that ν_n is determined by some vibrational mode in the solvation layer of the quenching anion, which destroys the activated complex configuration.[27] The stretching modes of water (symmetric and antisymmetric) have frequencies around 1.1×10^{14} s^{-1}, and that of the bending vibration is 4.8×10^{13} s^{-1}. Thus, they all have suitable frequencies and may contribute to ν_n. The following question now arises: Which of these factors is affected by the anions in a way that may account for the grouping? K_d is proportional to the square of the reaction distance[32] and therefore should follow the order $I^- > Br^- > Cl^-$ (assuming that in the three cases one water molecule separates M from X^-), i.e., opposite to that displayed by the intercepts. As for the water vibration frequencies, the effect of halides on the symmetric stretching was found to be small and little dependent on the nature of the anion,[33] again contrary to this argument. The other modes are not likely to behave differently, though this possibility cannot be ruled out. The electronic coupling, on the basis of its dependence on the separation of redox centers[27] and intensities of the charge-transfer bands,[34] is also expected to decrease from I^- to Cl^-, but there may be other parameters which reverse this order. In any case, we note that ν appears to be appreciably lower for reactions in group (a), for which the slope agrees with the theoretical value. For groups (b) and (c), the apparently high values of ν (subject to much uncertainty) may simply be associated with the approximations made in treating quenching in these groups as a full outer-sphere interaction.

C. Charge-Transfer Reactivity of $n\pi^*$ vs $\pi\pi^*$ Triplets. It is well established that $\pi\pi^*$ states of carbonyl triplets are much less reactive than $n\pi^*$ states in direct H-atom abstraction reactions, as typically observed with donors of high ionization potential and characterized by significant deuterium isotope effects.[35] It is also recognized that the transition state in such processes generally involves some degree of charge-transfer character, whose extent, in fact, is often measured by the quenching rate constant itself.[20,25] There appear to be varying opinions as to whether there is any intrinsic difference between $n\pi^*$ and $\pi\pi^*$ configurations in such charge-transfer interactions. Thus, on the basis of their detailed work on interactions of toluene and *p*-xylene with substituted phenyl ketones and other extended studies, Wagner et al. concluded that "it has not been established that there is any difference in (charge-transfer) reactivity between the two types of triplets".[36] However, Turro, reasoning from symmetry considerations, argues that "it is expected that electron abstraction, a reaction which possesses a topologically equivalent correlation diagram, should follow the same behavior qualitatively as hydrogen abstraction".[25] The problem of evaluating CT contributions to the rate of H-atom transfer reactions is further complicated by the possibility of overlapping reactions of close-lying or mixed $n\pi^*$ and $\pi\pi^*$ levels. Wagner et al. have therefore expressed the overall quenching rate as a weighted sum of direct $n\pi^*$ H-atom transfer and $n\pi^*$ and $\pi\pi^*$ CT contributions.[36]

Our results for anions which can function only as electron donors show clearly that there is no intrinsic difference between $n\pi^*$ and $\pi\pi^*$ triplets with respect to their CT quenching kinetics; both types follow the same log k_q vs $\Delta G^{\ddagger}$ correlations (Figure 2). Moreover, in agreement with Wagner et al.,[36] the results for anthraquinonesulfonates with 2-propanol (section IC) indicate that a rather small contribution of CT character to the triplet–quencher interactions is sufficient to weaken or eliminate the configurational selectivity in H-atom transfer, as far as the quenching rate constant is concerned. CT interactions tend to mask the effect of detailed electronic structure by emphasizing the overall thermodynamic properties. In this sense, the anthraquinones are not exceptional, and there is no need for ad hoc explanations such as the tunnel effect and the proximity of $n\pi^*$ and $\pi\pi^*$ levels (section IC), although these phenomena may still occur.

HCO_2^- and SO_3^{2-}. The rate constants for quenching of triplet AQ1S and AQ15DS by HCO_2^- were also measured (Table I) but are not included in Figure 2 because the reorganization energy $\bar{R}$ of HCO_2^- is not known. However, it is interesting to note the close values of $k_q(Cl^-)$ and $k_q(HCO_2^-)$ for both AQ2S and AQ1S, which supports the view that the *vertical* oxidation potentials of Cl^- and HCO_2^- are also close.[3] On the other hand, in the case of AQ15DS, $k_q(HCO_2^-)$ is appreciably higher than $k_q(Cl^-)$. Similar behavior has been observed for benzophenone-4-carboxylate (BC),[3] and here, too, some participation of proton transfer along the reaction coordinate may enhance the rate.[37] This is clearly supported by the isotope effect in quenching by formate: the measured values of k_H/k_D were 6.2, 2.1, and 1.1 for AQ15DS, AQ1S, and AQ2S, respectively (Table I, column 9).

Also measured was the quenching constant of SO_3^{2-} with AQ1S: $k_q = 3.1 \times 10^8$ M^{-1} s^{-1}. As in the case of AQ2S[1,2] and BC,[1,38] this puts SO_3^{2-} close to Br^- in its quenching rate constant, although its standard reduction potential (0.63 V) is much lower than that of Br^- (1.92 V).[8] This disparity again emphasizes the importance of the large reorganization energies in CT interactions involving small anions.[1]

III. Quantum Yields in Triplet AQS–Anion Interactions. Contrary to the chemical inertness of the weak anthraquinone sensitizers in H-atom abstraction (section IC), they are as efficient as the strong ones in their CT interactions with anions. In this section, we show that the dependence of bulk radical yield from triplet AQ1S and AQ15DS on both the identity and concentration of the quenching anion follows in detail the same patterns as are observed for AQ2S[2] or BC.[38] It is helpful first to review this pattern.

(32) A more accurate value of K_d can be calculated by Eigen's equation (Eigen, M. *Z. Phys. Chem. (Leipzig) NF1* **1954**, 176). For zero Coulombic interaction and reaction distance of 7.3 Å,[1] this equation gives $K_d = 0.94$.
(33) Dwivedi, P. C.; Rao, C. N. R. *Spectrochim. Acta* **1970**, *26A*, 1533.
(34) The oscillator strength of the CTTS bands increases in the order: $Cl^- < Br^- < I^-$ (Jortner, J.; Treinin, A. *Trans. Faraday Soc.* **1962**, *58*, 1503.)
(35) Wagner, P. J. *Top. Curr. Chem.* **1976**, 66. Scaiano, J. C. *J. Photochem.* **1973**, *2*, 81.
(36) Wagner, P. J.; Truman, R. J.; Puchalski, A. E.; Wake, R. *J. Am. Chem. Soc.* **1986**, *108*, 7727.
(37) The intermediate formation of the protonated radical was not observed (see Section III).
(38) Hurley, J. K.; Linschitz, H.; Treinin, A. *J. Phys. Chem.* **1988**, *92*, 5151.

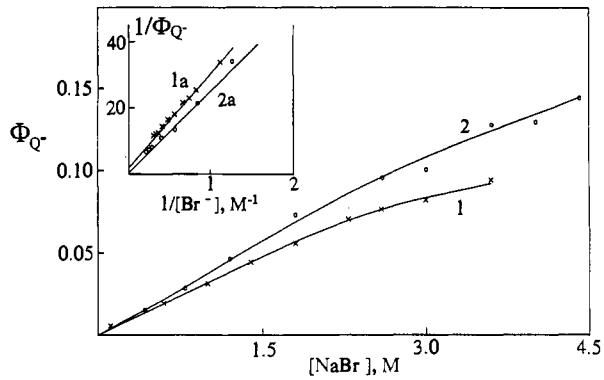

Figure 3. Interaction of AQ1S and AQ15DS triplets with Br^-. Dependence of quantum yield of semiquinone on $[Br^-]$. Curve 1: 2.4×10^{-4} M AQ1S + 10^{-2} M phosphate buffer, measured at 500 nm. Curve 2: 4×10^{-4} M AQ15DS, 510 nm. All samples were air-free. Inset: dependence of ϕ_R^{-1} on $[Br^-]^{-1}$ for AQ1S (1a) and AQ15DS (2a).

With regard to their reactions with organic triplets, ^3M, inorganic anions fall into two groups. Group I includes halides and pseudohalides, for which radical formation ($M^{\bullet-}$ and $X_2^{\bullet-}$) occurs only at anion concentrations higher ($[X^-] > 0.1$ M) than that required to quench most triplets ("R branch" of ϕ_R vs $[X^-]$ plot). Any reactions of the triplet with water (k_W) are quenched competitively by these anions at low concentration ("Q branch") without radical production. Group II ions, including NO_2^-, SO_3^{2-}, and HCO_2^- (the case of N_3^- is discussed separately), reduce triplets efficiently, forming radicals in the quenching process at low $[X^-]$. (In some NO_2^-–organic triplet pairs, energy transfer is more exoergic than charge transfer, and this competing process can also suppress radical production.[1]) The following somewhat simplified general scheme represents the situation where energy transfer does not interfere.[2,38]

Scheme II

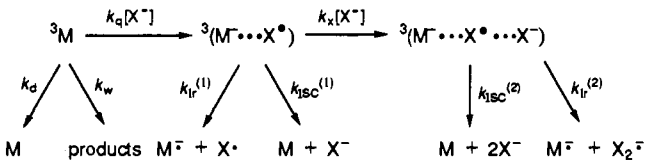

The behavior of Group I ions at low $[X^-]$ is explained by taking $k_{ISC}^{(1)} \gg k_{fr}^{(1)}$ in consequence of strong spin–orbit coupling in the incipient radical component ($X^\bullet$) of the primary exciplex ("IRSOC model").[39] At high $[X^-]$, formation of a termolecular exciplex in which $X_2^{\bullet-}$ has low SO coupling permits separation of the final radical pair. In agreement with experiment, this leads, in the high $[X^-]$ region, to linear plots of ϕ_R^{-1} vs $[X^-]^{-1}$, with slope $k_{ISC}^{(1)}/\theta_R k_X$, where θ_R is the fractional radical yield from the ternary exciplex.[2,38]

The behavior of Group II anions is explained by *low* SO coupling in the radical formed by oxidation. Thus, $k_{fr}^{(1)} \gtrsim k_{ISC}^{(1)}$, and radicals are formed readily in the primary quenching step, at low $[X^-]$. The yield remains high, with increasing $[X^-]$.

Group I Reactions. Figure 3 shows the variation of ϕ_R (measured for the organic radical) with $[X^-]$ along the R branch for the interaction of Br^- with triplet AQ1S and AQ15DS. In the Q region, at $[Br^-]$ below 0.2 M, ϕ_R is essentially zero, corresponding to absence of a water reaction and quenching with high $k_{ISC}^{(1)}$. For $[Br^-] \geq 0.2$ M, the yield rises for both AQ1S and AQ15DS, as typically observed for Group I anion interaction with AQ2S[2] and BC,[38] and linear plots of ϕ_R^{-1} vs $[Br^-]^{-1}$ are obtained (Figure 3, inset).

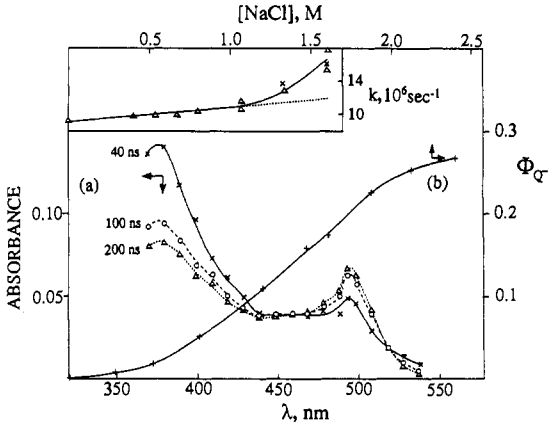

Figure 4. Interaction of triplet AQ1S and Cl^-. Time evolution of transient absorption spectrum in 2 M NaCl, and the dependence of quantum yield of semiquinone (measured at 500 nm) on $[Cl^-]$; $[AQ1S] = 1 \times 10^{-4}$ M. Inset: dependence of pseudo-first-order rate constants of triplet decay (Δ, 380 nm) and semiquinone growth (×, 500 nm) on $[Cl^-]$; $[AQ1S] = 2.4 \times 10^{-4}$ M. All samples were air-free and contained 10^{-2} M phosphate buffer (pH 7.5).

Table II. Group I Anions: Parameters of Linear Correlations, ϕ_R^{-1} vs $[X^-]^{-1}$ in R Branch Region and Maximum Observed ϕ_R[a]

X⁻	NQ	AQ2S[d]	AQ1S	AQ15DS	BC[e]
		LImiting Yields, ϕ_R^{∞}[b] and Slopes (M)[c]			
Cl^-	0.5 (5.7)	0.51 (0.50)	~0.5[f]		
Br^-	0.2 (35)	0.2 (21)	~0.5 (29)[g]	~0.8 (25)[g]	0.16 (7.6)
I^-		0.1 (28)			0.2 (78)
SCN^-	0.20 (4.3)	0.51 (1.6)	0.46 (2.7)		0.60 (1.8)
		ϕ_R^{max}(obs)[h]			
Cl^-	0.17 (3.5)*	0.51 (1.5)	0.27 (2.4)*		
Br^-	0.06 (4.8)*	0.10 (3)	0.10 (3.6)	0.14 (4.4)*	0.13 (5)*
I^-		0.07 (5)*	*i*		0.06 (6)*
SCN^-	0.17 (4.5)*	0.51 (6)	0.35 (3.8)*		0.50 (6)*

[a] Radical yield of reduced species. Unless otherwise stated, results from present work. [b] The limiting quantum yield is given by the reciprocal of intercept. [c] Recorded in parentheses. According to the proposed mechanism, slope = $k_{ISC}^{(1)}/k_x\theta_R$. [d] From ref 2, corrected for revised actinometry. [e] Reference 38. [f] From a plot of $\theta q/\phi_R$ against $1/[X^-]$, where θq is the fraction of triplets quenched (since the Q and R branches overlap). [g] Considerable uncertainty because of small intercepts. [h] Highest quantum yield measured. In parentheses, the corresponding X^- concentration (M). The asterisk signifies that the yield still increases with $[X^-]$. [i] $\phi_R = 0.07$ at 4 M I^-, but above 2 M thermal reactions were observed.

The situation for the interaction of Cl^- with AQ1S and AQ15DS (Figure 4) is somewhat complicated by the relatively low primary quenching rate, k_q, which leads to both an overlap of the Q and R branches of the ϕ_R vs $[Cl^-]$ plot and an increase of k_q at high $[Cl^-]$, as noted above (Figure 4, inset). The latter probably results from a "nearest neighbor effect",[40] which operates only at high quencher concentration, perhaps augmented by an effect of ionic strength on the reaction between similarly charged molecules. However, the sigmoid shape of ϕ_R vs $[Cl^-]$ (Figure 4b) is only partly due to the increase in k_q with $[Cl^-]$, in competition with k_d (Scheme II): a considerable rise of ϕ_R occurs already in the region where k_q is constant (up to ~1.1 M), and its overall increase is much larger than that resulting simply from increasing k_q. Figure 4 also shows the evolution of the transient spectrum, from triplet to radical, well into the R branch (2 M Cl^-). The final product is the semiquinone anion $AQ1S^{\bullet-}$, clearly identified by its two intense bands around 400 and 500 nm and its fast reaction with O_2.[5] The somewhat higher intensity of the 400-nm band is due to overlap with Cl_2^- absorption.[2,7] The rate constants of $AQ1S^{\bullet-}$ *formation*, measured at 500 nm for two Cl^- concentrations, were found to be the same (within limit of error) as the

(39) Treinin, A.; Loeff, I.; Hurley, J. K.; Linschitz, H. *Chem. Phys. Lett.* **1983**, *95*, 333.

(40) Wagner, P. J. *J. Am. Chem. Soc.* **1967**, *89*, 5715. Keizer, J. *J. Am. Chem. Soc.* **1983**, *105*, 1494.

Table III. Group II Anions: Maximum Radical Quantum Yields[a]

anion	NQ	AQ2S	AQ1S	AQ15DS	BC
NO_2^-	0.97[b]	0.81[b]	≥0.50 (0.05) 0.50[c]	0.74[c]	0.05[b,d]
SO_3^{2-}		0.8[b]	0.45 (0.5–1)[e]		0.6 (0.4–0.8)
HCO_2^-[f]	0.77[h]	0.32[g]	0.31[c,h]	~0.27[i]	0.73[g,j]
N_3^-	0.07 (0.1–0.2)	0.13 (0.05–0.2)	0.02 (0.2–2)	0.04 (0.1–2)	~0.01[k]

[a] Radical yield of reduced species. In parentheses, corresponding range of anion concentration (M) where ϕ is constant or highest concentration employed if $\phi \leq \phi^{max}$. Unless otherwise stated, results from present work. [b] Reference 1. [c] From intercept of linear correlation between θ_q/ϕ and $[X^-]$ (see ref 1). [d] Energy transfer is more efficient. [e] ϕ_R starts to decrease above 1 M. [f] Primary quantum yields (first stage, see text). [g] Reference 3. [h] The overall yield was determined and divided by 2 (see text). [i] Determined at a time when the two absorption bands around 400 and 500 nm have nearly the same intensity (see footnote 43). [j] H-transfer occurs as first stage. [k] Reference 38.

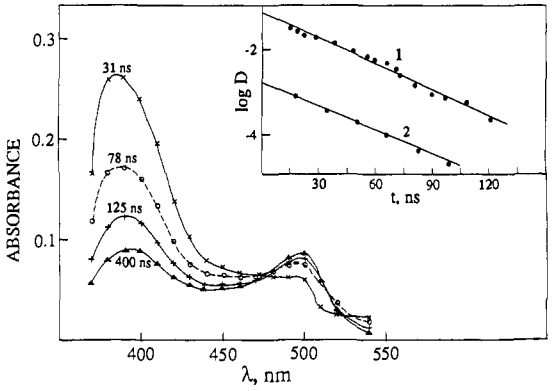

Figure 5. Interaction of triplet AQ1S with NO_2^-. Time evolution of transient absorption spectrum in air-free solution containing 2.4×10^{-4} M AQ1S with 10^{-2} M $NaNO_2$. Inset: first-order plots for triplet decay measured at 390 nm (1) and for growth of semiquinone, 500 nm (2).

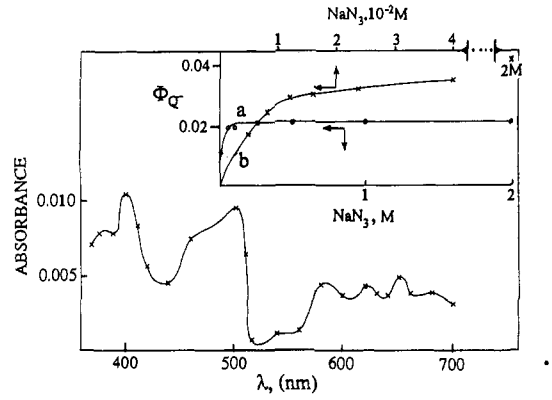

Figure 6. Interaction of AQ1S and AQ15DS triplets with N_3^-. Transient absorption spectrum produced in air-free solution containing 2.4×10^{-4} M AQ1S + 2 M NaN_3, 4 μs after pulse. Inset: dependence of quantum yield of semiquinone on $[N_3^-]$ for AQ1S (curve a, measured at 500 nm) and AQ15DS (curve b, 510 nm).

corresponding constants of triplet decay (see inset). This provides further evidence that the production of free radicals at high anion concentrations is initiated by interactions of X^- with the lowest triplet and not with some precursor (e.g., excited singlet S_1 or ground-state EDA complex).[38] Similar behavior is observed for AQ15DS.

Linear double reciprocal plots (ϕ_R^{-1} vs $[X^-]^{-1}$) analogous to those in Figure 3 have been obtained for the interaction of other triplets with Group I anions. Table II summarizes the parameters of these lines, as derived from the present work and previous studies (see footnotes to Table II). Included in the table are the limiting yields, ϕ_R^∞, extrapolated to infinite $[X^-]$ (reciprocals of intercepts), and the yields actually observed at the highest anion concentrations used, ϕ_R^{max}(obs). In several cases (including systems of the weak sensitizers), the difference between these two yields is large, even when the data lead to reasonably straight lines. This suggests that some deactivation process (e.g., interaction with the singlet excited state) occurs at high anion concentrations, which makes the intercepts less significant as limiting yields. But even if we confine ourselves to values of ϕ_R^{max}(obs), it is clear that there is no systematic difference between strong ($n\pi^*$) and weak ($\pi\pi^*$) sensitizers in efficiency of radical formation following quenching by Group I anions.

Inspection of Table II indicates the following: (a) In all cases the slopes increase in the order $SCN^- \sim Cl^- < Br^- < I^-$, corresponding to the order of spin–orbit coupling ζ_X in the radical X, i.e., the order of $k_{ISC}^{(1),2}$ (b) values of ϕ_R^{max} are less sensitive to the nature of the anion, but they tend to increase as ζ_X *decreases*. This may reflect some residual spin–orbit coupling in the *dianion*, X_2^- (probably gained by configuration interaction of ground state with excited states), which should affect θ_R. (c) Strong and weak sensitizers display similar slopes and yields; in this respect, too, $n\pi^*$ and $\pi\pi^*$ electronic configurations behave similarly.

Group II Reactions. The reduction of triplet AQ1S to its radical anion by NO_2^- is shown in Figure 5. At $[NO_2^-] = 0.01$ M, the triplet is 53% quenched. The semiquinone anion grows in at the same rate as triplet decay (inset, Figure 5), with the pseudo-first-order rate constant k(growth) = 1.9×10^7 s^{-1}, in agreement with measured values of k_d^T (9×10^6 s^{-1}) and k_q (1.0×10^9 M^{-1} s^{-1}) (section IA and Table I).

The other typical characteristics of Group II anion quenching including absence of an R branch, as observed in all systems studied to date, are found here also for both AQ1S and AQ15DS. The radical yield increases with anion concentration up to a limiting value corresponding to practically complete quenching and then remains constant over a considerable concentration range (see, e.g., Figures 5–7 in ref 1).[41] Beyond this range, decline of ϕ_R with increasing concentration was observed in some cases (e.g., AQ1S/SO_3^{2-} above 1 M), which may be due to quenching of the primary exciplex.[1,2] (Singlet quenching may also contribute at high concentrations.) All relevant data from this and previous works are collected in Table III.

Azide represents an intermediate case between Groups I and II. The quantum yields at total quenching are rather low (Table III), and in the case of BC the resemblance to Group I is further indicated by a slowly rising R branch.[38] This behavior is in accord with two properties of the azide radical: (i) its spin–orbit coupling is low but appreciable (π-state) and (ii) like other Group I anions, its radical can form a dianion, X_2^-, though the stability constant of N_6^- is relatively small.[42] Indeed, the formation of N_6^-, which was observed with the BC/N_3^- system,[38] is also seen here for AQ1S + 2 M N_3^- (Figure 6). In addition to the double-peaked spectrum of $AQ1S^{\bullet-}$, there is an ill-defined but clearly present absorption around 620 nm (λ_{max} of N_6^-, 645 nm[42]). However, no R branch was observed with AQ1S and AQ15DS; from 0.1 M up to 2 M, ϕ_R remains constant (Figure 6, inset). Furthermore,

(41) With some NO_2^- and HCO_2^- systems the maximum yields were not reached because of limitations imposed on raising $[X^-]$. This limitation was due to laser light absorption by NO_2^- (ϕ_R was corrected for inner filter effect, but this correction did not exceed ~10%) or to the low quenching rate constant of HCO_2^-. In these cases, the dependence of θ_q/ϕ_R on $[X^-]$ was used to derive ϕ_{max}. This method also corrects for exciplex quenching (see ref 1).

(42) Butler, J.; Land, E. J.; Swallow, A. J. *J. Radiat. Phys. Chem.* **1984**, *23*, 265.

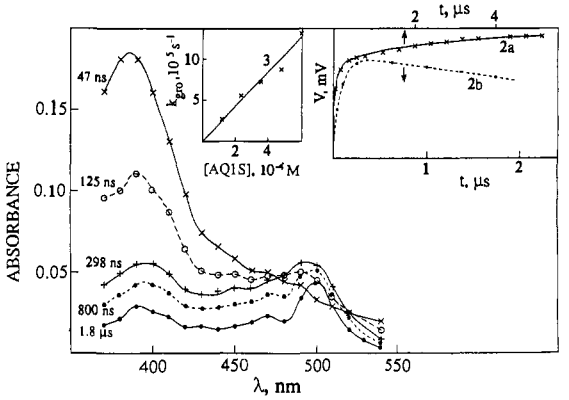

Figure 7. Interaction of AQ1S with HCO_2^-. Time evolution of transient absorption spectrum in O_2-saturated solution containing 2.4×10^{-4} M AQ1S + 2 M HCO_2Na. Inset 2 (right): kinetic traces for semiquinone at 500 nm in air-free (2a) and O_2-saturated (2b) solutions containing 2×10^{-4} M AQ1S + 2 M HCO_2Na. Inset 3 (left): dependence of pseudo-first-order rate constant of semiquinone growth (secondary reduction) on [AQ1S], measured at 500 nm.

with AQ2S and NQ, the R branch is replaced by a decline of ϕ_R with increasing $[N_3^-]$, which was attributed to quenching of the primary exciplex.[2] In general, the behavior of azide systems at high N_3^- concentrations appears to depend on the outcome of the Q branch, i.e., on its ϕ_R^{max}. As the latter decreases, the high-concentration branch changes its direction from upwards (i.e., R branch) to downwards, with AQ1S and AQ15DS holding a middle position (no change). A detailed analysis of this behavior, based on the properties of the azide radical, is presented in ref 38.

The interaction of HCO_2^- with triplet AQ1S, while initially slower than that with AQ2S or NQ (Table I), proceeds similarly in two stages:[3] reduction occurs, first by HCO_2^- and then by $CO_2^{\bullet-}$ (produced from the radical $HCO_2^\bullet$). This is shown in Figure 7 (kinetic trace 2a, inset). From the effect of AQ1S concentration on rate of the secondary reaction (inset 3a), the rate constant of

$$AQ1S + CO_2^{\bullet-} \rightarrow AQ1S^{\bullet-} + CO_2 \qquad (7)$$

was determined: $k = 2.1 \times 10^9\ M^{-1}\ s^{-1}$. (A previous result obtained by pulse radiolysis is $3.3 \times 10^9\ M^{-1}\ s^{-1}$.[5]) In O_2-saturated solutions, only the first reduction stage occurs (kinetic trace 2b), since $CO_2^{\bullet-}$ is preferably scavenged by O_2 under the conditions employed.[3] The corresponding transient spectral evolution shows the gradual formation of semiquinone anion in parallel with triplet decay (Figure 7). The ratio between the two contributions to the total quantum yield ϕ_R could be determined as previously described[3] from the analysis of kinetic traces or from the effect of O_2, but the relative contribution of the second stage, which was found by this method, was only ~60%. Similar discrepancies were observed with AQ2S and BC,[3] the reason for which is not clear.[43]

As previously noted (Section IIB), the kinetics of quenching by formate, including marked isotope effects, strongly suggest that substantial H-movement or even H-abstraction may be involved in the primary process for AQ15DS and apparently also for AQ1S. Nevertheless, as in the case of AQ2S,[3] transient spectra observed shortly after the flash[44] in solutions of AQ1S or AQ15DS with HCO_2^- show no indication of H-abstraction (formation of acidic semiquinone) preceding the production of the radical anion by deprotonation. However, deprotonation by formate itself[3] may be too fast to be detected by our equipment, in particular when $[HCO_2^-]$ is above ~0.5 M, as required by the weak sensitizers in order to obtain appreciable quenching. Indeed, in the BC/HCO_2^- system, the protonated semiquinone is clearly identified as the primary product of triplet quenching.[3] In this instance (and probably for triplet AQ15DS), the high efficiency of H-atom abstraction, mediated by charge transfer, is at variance with a previous generalization that the "maximum quantum efficiency for radical production (in H-abstraction reactions) is lowered for both $n\pi^*$ and $\pi\pi^*$ triplets whenever thermodynamics favors significant electron transfer during CT complexation" [36] (attributed to efficient back electron transfer competing with proton transfer[25]).

From Table III we can draw the following conclusions concerning ϕ_R in direct reduction of triplets by Group II anions: (a) there is no clear-cut difference between $n\pi^*$ and $\pi\pi^*$ configurations and (b) with some irregularities, there is a tendency for ϕ_R to increase as $\Delta G°_{CT}$ decreases, i.e., as the exciplex approaches more closely the pure CT state and becomes more prone to dissociation into its radicals. This point was discussed elsewhere,[3] but it is clear from the irregularities that other factors should be considered. Among them is the effective rate of deactivation, which takes into account k_{ISC} and the energy gap between triplet and ground state (see ref 3). This energy gap decreases with more favorable $\Delta G°_{CT}$, which leads to the opposite effect of $\Delta G°_{CT}$ on ϕ_R.

In conclusion, these results define the range of validity for treatment by Marcus theory of CT reactions of simple anions with organic triplets, using spectroscopically derived reorganization energies of the anions. Systematic deviations from the theoretical behavior suggest partial electron transfer in the reaction complex. These CT interactions show no significant configurational selectivity. Both quenching kinetics and radical yield depend not on whether the organic triplet is in an $n\pi^*$ or $\pi\pi^*$ state but mainly on its thermodynamic properties. As for H-abstraction via a CT intermediate, the situation with regard to ϕ_R is rather ambiguous. If triplet AQ15DS ($\pi\pi^*$) indeed abstracts H-atom from HCO_2^-, then there is no essential difference between its effectiveness in this regard and that of BC ($n\pi^*$) (Table III). On the other hand, ϕ_R values from the interactions of anthraquinone triplets with 2-propanol indicate distinct selectivity: $^3n\pi^*$ states are much more efficient than $^3\pi\pi^*$. Possible reasons for this have been briefly cited above (Section IC).

Acknowledgment. We much appreciate support of this work by the U.S. Department of Energy, Division of Chemical Sciences, Office of Basic Energy Sciences (Grant 89ER14027, to Brandeis University), and by the U.S.–Israel Binational Science Foundation (Grant 84-00026, to the Hebrew University of Jerusalem). The Farkas Center is supported by Bundenministerium für Forschung and Technologie and the Minerva Gessellschaft für die Forschung.

(43) The behavior of AQ15DS was found to be more complicated. The intermediate produced in the second stage is not the semiquinone but an unidentified species with $\lambda_{max} \sim 500$ nm (no twin peak at ~400 nm which characterizes the semiquinone) and whose formation is not prevented by O_2 or accelerated by OH^- (i.e., no deprotonation is involved).

(44) Reliable measurements were taken only after ~20 ns following the flash.